Control of a Semi-Circular Planform Wing in a "Gusting" Unsteady Freestream Flow: I – Experimental Issues

David R. Williams[1] and Jesse Collins[2]
Illinois Institute of Technology, Chicago, IL, 60616

Gilead Tadmor[3]
Northeastern University, Boston, MA, 02115

and

Tim Colonius[4]
California Institute of Technology, Pasadena, CA, 91125

Active flow control is used to modify the lift, drag and pitching moments on a semi-circular wing during "gusting" flow conditions. A longitudinal oscillating flow component has an amplitude of 10 percent of the freestream speed and a frequency giving k = 0.048 (f =0.2 Hz). The aspect ratio of the wing is AR = 2.54, and the chord Reynolds number of the wing is 70,600. Pulsed-blowing flow control actuation occurs along the leading edge of the airfoil via 16 spatially localized micro-valve actuators. Feed-forward control based on a quasi-steady lift model is used to stabilize lift fluctuations generated by an oscillating free stream, which simulates the longitudinal component of a gusting flow. The quasi-steady system model reduces the amplitude of the fundamental and first harmonics of lift oscillations, but does not account for time delays. The time delay between the lift and the freestream oscillation was measured to be $\tau_u^+ = 4.8$. The time delay between the lift and the actuator input signal was found to be $\tau_a^+ = 11.3$.

Nomenclature

A	=	amplitude of lift coefficient oscillation
C_μ	=	momentum coefficient of pulsed blowing actuator, $\frac{\dot{m}_{jet} u_{jet}}{\rho U_0^2 S}$
C_L	=	lift force coefficient
c	=	chord along centerline of the wing
f	=	fundamental frequency of oscillation
k	=	reduced frequency, $\frac{2\pi fc}{U_0}$
S	=	planform area of wing
U_0	=	mean freestream speed
U_∞	=	instantaneous freestream speed - $U_\infty(t) = U_0 + U'(t)$
U'	=	instantaneous freestream speed fluctuation
α	=	angle of attack
γ	=	coherence function
τ_a, τ_a^+	=	lift time delay relative to actuator input, and normalized form
τ_u, τ_u^+	=	lift time delay relative to flow speed changes, and normalized form

[1] Professor, MMAE Dept., 10 W. 32nd St., AIAA associate fellow.
[2] Graduate Research Assistant, MMAE Dept., 10 W. 32nd St., AIAA student member.
[3] Professor, Electrical and Computer Engineering Dept., and AIAA member.
[4] Professor, Mechanical Engineering Dept., and AIAA senior member.

I. Introduction

A principal objective of our MURI research program (discussed by Colonius[1]) is to use active flow control as an "inner-loop" controller, to modify the larger scale flight dynamics (outer loop) of a low aspect ratio wing. On conventional aircraft the ailerons and flaps are used to change the lift and drag coefficients in response to changing flight conditions, which is outer-loop flight control. Using the inner-loop active flow control, we are able to modify the lift, drag, and pitch moment coefficients by changing the flow state without changing the physical geometry of the wing, see Ref.2. Our earlier work has shown that we can modify the strength of the vorticity near the leading edge of the wing when it is at high angles of attack. This produces higher lift coefficients, consistent with the large body of work on active flow control for separation control and lift enhancement. The current focus is to enhance wing maneuverability using only the inner-loop flow control to modify the outer "flight control" loop. To do this requires an understanding of the coupling between the two control loops. In particular, an understanding of the time lags in the flow field in response to changes in actuation, and the time response of the lift to changing flight conditions are parameters that are just as important as the frequency response between actuator input and lift force output.

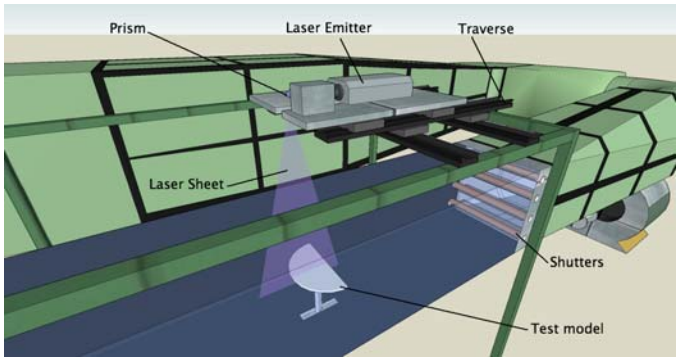

Fig 1. IIT – Fejer unsteady flow wind tunnel showing PIV system arrangement.

In this experiment we examine the ability of inner-loop flow control to modify the lift force on a wing in an unsteady flow field. The unsteady flow is a simple sinusoidal oscillation of the freestream speed about a mean value, which produces an oscillating lift force through the changing dynamic pressure. The oscillating flow is meant to simulate one frequency in the spectrum of longitudinal gust fluctuations (see Hoblit[3].) The outer-loop control objective is simply to maintain a constant lift force on the wing in the unsteady flow. The inner-loop control objective is to change the lift coefficient in a way to offset the lift force fluctuations arising from the oscillating freestream, and demonstrate the feasibility of changing the lift coefficient in a *time varying manner* to compensate for unsteady flow effects. This is a departure from the historical approaches to flow control, which typically attempt to maximize changes in lift with a minimal amount of actuator power.

In this paper we will demonstrate the use of flow control to modulate the strength of the leading edge vortex in response to an unsteady freestream flow simulating wind gusts. We describe the use of a feed-forward controller designed to model plant dynamics based on a quasi-steady assumption. A hotwire probe provides measurements of the freestream oscillations to drive the flow control actuators in the correct manner to achieve the desired C_L fluctuation based on the system model.

II. Experimental Setup

The experiments are being conducted with a low aspect ratio wing under both steady and dynamic conditions in the Andrew Fejer Unsteady Flow Wind Tunnel shown in Fig. 1. The chord Reynolds number for the current set of data was acquired at Re_c = 70,600 when the freestream speed is U_0=5.25 m/s. A computer controlled shutter mechanism at

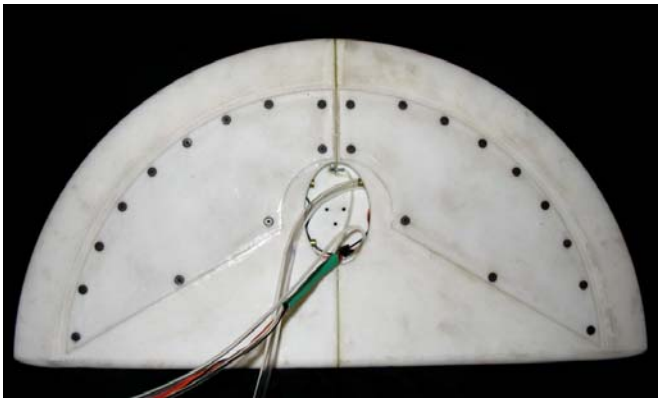

Fig. 2 – Bottom view of the 3D airfoil model showing the force balance mounting holes (center 3 holes), air supply lines, micro-valve and pressure transducer connections.

the downstream end of the test section allows the freestream speed to be modulated at frequencies up to 3 Hz, although the majority of the results presented in this paper were acquired at 0.2Hz. The model is mounted on a two-component vertical sting, controlled by Xenus servotubes. The height, pitch angle and pitch rate of the model within the test section are computer controlled in response to the instantaneous loads acting on the wing. The response of the model is controlled by a dSPACE 1102 system, which contains a second-order differential equation model for the wing. With this system it is possible to simulate complex flight maneuvers.

A photograph of the bottom of the airfoil model used in the experiments is shown in Fig. 2. The planform is a semi-circle with a centerline chord C = 203mm, and span b = 406mm giving an aspect ratio $=b^2/S= 2.54$. Sixteen micro-valves for pulsed-blowing actuation are installed internally along the leading edge of the wing, similar to the approach used in Williams, et al[4]. Two pressurized air plenums are built into the wing, which supply the micro-valves. At this stage in the project all actuators are driven in-phase, but they can be individually controlled to produce a roll moment. Under normal operating conditions, such as to document the open-loop forcing effects on performance, the actuators are operated at 25 Hz pulse rate, with a momentum coefficient $C_\mu = 0.0074$.

III. Results from Open Loop Forcing Tests

The steady state lift and drag forces as well as pitch moment about the aerodynamic ($x_{ac}/c = 0.37$) center acting on the semi-circular wing are shown in Fig. 3 with and without leading edge actuation. The effect of the actuation is to delay stall beyond $\alpha = 15^o$ and to produce a larger $C_{Lmax} = 1.2$ just prior to stall. The range of lift control available at $\alpha = 19^o$ is indicated by the dashed lines in Fig. 3a,b, and c. Actuation increases the drag force as well as the lift, which can be seen in Fig. 3a, and b. When the wing is placed in a gusting flow field at a fixed angle of attack, then the controller will take advantage of its ability to modify the lift force, and attempt to suppress lift oscillations.

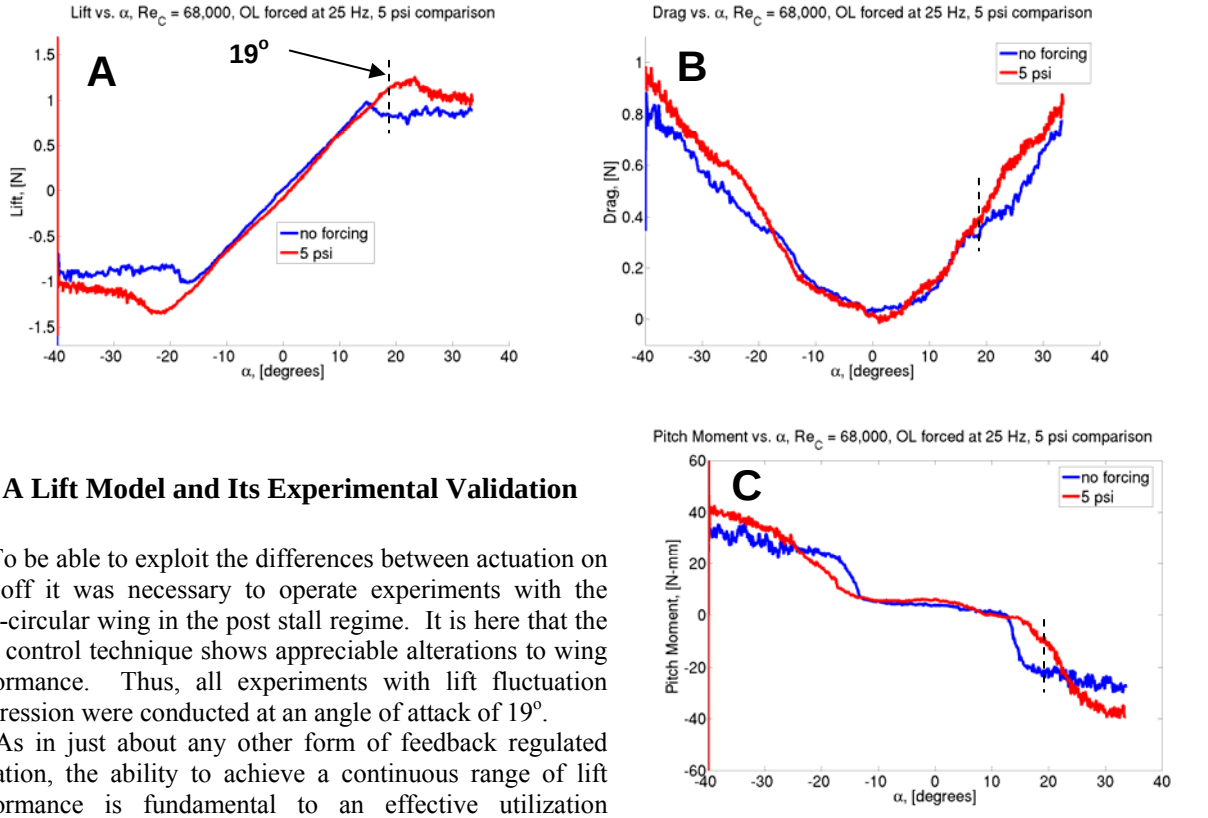

Figure 3. Lift, drag, and pitch moment dependencies on angle of attack for the forced and unforced cases, $Re_C = 68{,}000$.

IV. A Lift Model and Its Experimental Validation

To be able to exploit the differences between actuation on and off it was necessary to operate experiments with the semi-circular wing in the post stall regime. It is here that the flow control technique shows appreciable alterations to wing performance. Thus, all experiments with lift fluctuation suppression were conducted at an angle of attack of 19^o.

As in just about any other form of feedback regulated actuation, the ability to achieve a continuous range of lift performance is fundamental to an effective utilization feedback flow control. While it is possible to change the momentum coefficient of the actuator by modulating the blowing pressure amplitude, this turns out to be rather ineffectual, primarily due to the long time response associated with the plenum in the wing, but also due to hardware limitations. Instead we opt here for using duty ratio

modulation under a constant supplied pressure. This is a common option where a constant power source is a defining factor. The control by use of solid state switches of electric power converters and inverters, with a constant, dc source, is a ubiquitous example. Actuation policies are thus defined in terms of two constant and one time varying quantities. Specifically,

1. The length of a single square wave blowing period T_B: Under actuation command at the time $t_k=kT_B$, the valves are open during $[kT_B , (k+0.5)T_B]$, and are closed during $((k+0.5)T_B , (k+1)T_B)$.
2. The modulation period of L blowing cycles (i.e., time intervals of length LT_B). The essence of the duty ratio control is the determination of during how many and which of the L blowing periods will actual blowing occur. This is the purpose of the time varying control command and the essence of control design in our system.

Figure 4 shows a calibration of the control increment to the lift coefficient, denoted here by ΔC_L. To allow both positive and negative modulation we shall use a fixed baseline duty ratio as the origin. The results in that figure are based on L=15, allowing 16 quantization levels for the continuous duty ratio range of 0% – 100%. The figure shows both the discrete experimental evaluations (the red, rectilinear curve) and a continuous approximation (the blue curve).

A quasi-steady model equation was used for the feed-forward control. Feed-forward control is characterized by system plant knowledge used to exert to a corrective measure. It is not a self-correcting control however, and thus the actuated system is susceptible to errors due to incomplete plant knowledge, including the highly simplified representation of the actuator and its effect, sensor noise, disturbances and ignored actuation and sensing delays. The system plant is based on the ideal steady state model of the lift coefficient shown in Eq. (1).

$$C_L = \frac{L}{\frac{1}{2}\rho U_\infty^2 S} \tag{1}$$

Next we assume that $U_\infty(t)$ and $C_L(t)$ are time dependent quantities. We assume that the varying quantities (U_∞, and C_L) will be changing in time, but slowly enough that the semi-circular wing lift generation can "quickly" adjust to these changing quantities. While we use this model in inherently time varying experiments, where U_∞ and C_L are changing in time, we shall only address here the case where the time constant of both the natural and actuated lift response are sufficiently fast to justify the quasi steady-state appeal to equation 1, assuming and instantaneous lift response. The validity of this assumption is explored at the end of this paper, by varying the frequency of the freestream oscillation and measuring the phase delay.

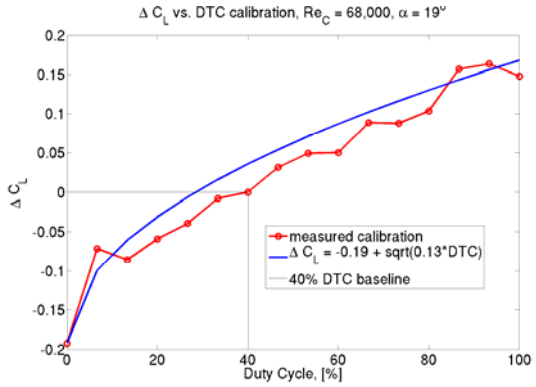

Figure 4. ΔC_L vs. Duty cycle calibration

To continue the derivation of the output equation we rearrange equation 1 in a way that distinguishes faster and slower fluctuations in U_∞ and C_L, and introduce the notations.

$$U_\infty = U_0 + U' \qquad C_L = C_{L0} + C_L' \qquad L = L_0 + L' \tag{2a,b,c}$$

In line with common conventions, the slowly varying mean component is denoted by a "naught" subscript, and the zero mean fluctuating component is denoted by a "prime" superscript. Substitutions into Eq. 1 result in the following:

$$\frac{2}{\rho S} L_0 = C_{L0} U_0^2 \qquad \frac{2}{\rho S} L'(t) = C_L'\left(U_0^2 + 2U_0U' + U'^2\right) + C_{L0}\left(2U_0U' + U'^2\right) \tag{3a,b}$$

Equation 3b quantifies fluctuations in the lift output, L(t), as a function of fluctuations in the incoming flow (viewed as an exogenous input) and the actuated changes in the lift coefficient. We group the various terms in Eq. 3, separating altogether the constant term that contributes only to the mean lift. Terms that involve only a single fluctuating component contribute to the fundamental frequency in response to oscillatory variations in the input. Likewise, quadratic and cubic fluctuation terms determine higher output harmonics, but their contributions relative to the dominant fundamental are negligible when the input fluctuations are relatively small.

To evaluate the accuracy of the output equation 3, preliminary tests were conducted where only a single quantity is allowed to oscillate at a time. This causes equation 3 to simplify substantially. First demonstrated is the case of freestream oscillations: $U_\infty = 5.25 + 0.25\cos(\omega t)$ characterized the free stream oscillations. Because the lift force is proportional to the dynamic pressure, without lift suppression from the actuators, an oscillatory lift signal is expected as shown in Eq. 4. Equation 4 is the simplified form of Eq. 3 with all C'_L terms removed because the lift coefficient is not allowed to change (that is, without pulsed blowing actuation).

$$L(t) = \frac{\rho S}{2}\left[C_{Lo}U_o^2 + \underline{2C_{Lo}U_oU'} + \underline{\underline{C_{Lo}U'^2}}\right] \tag{4}$$

Figure 5 compares the measured lift force time series and spectra from the wing with the prediction by Eq. 4. The values of $C_{L0} = 1.0$, $U_0 = 5.25$m/s and U'=0.25m/s were used for the data shown. The instantaneous $U_\infty(t)$ is provided by a hot wire anemometer. Due to the presence of the U^2 term in the dynamic pressure, a first harmonic term is present in the output of Eq. 4.

The first order fundamental frequency is 25dB stronger than the second order harmonic, and thus the harmonic term

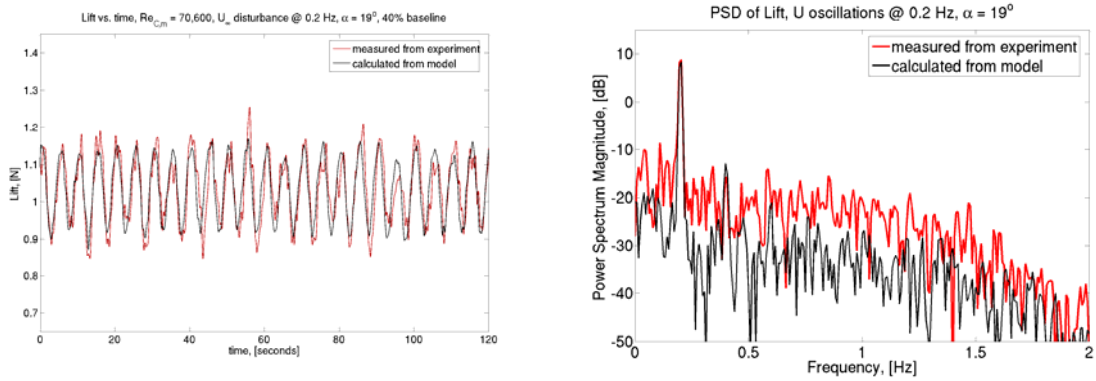

Figure 5. Time series (a) with spectra (b) of lift from experiment and Eq. 4 lift prediction for freestream oscillation.

is not easily distinguishable in the spectrum. Measurements of the coherence between the lift force and the freestream speed show a very high correlation ($\gamma = 0.9$) at f = 0.2 Hz and 2f = 0.4 Hz. The higher broadband noise levels measured by the experiment

The apparent agreement between the model and measurements of the amplitude and the frequency is encouraging, and suggests the quasi-steady lift model is valid for this flow. The two time series signals also are closely aligned in phase, showing that the quasi-steady assumption is valid for the utilized frequency. There are some noisy peaks in the experiment, however overall the agreement is good.

The second case test of Eq. 3 is to keep the freestream speed constant (U'=0) and to vary the lift coefficient, C_L'. In this case, U_∞ is a constant, and the duty cycle to the pulsed-blowing jets is varied. We attempt to produce a sinusoidal lift oscillation by changing $C'_L(t)$ using active flow control. Due to the non-linearity of the duty cycle calibration to C'_L, visualized in Figure 4, the mapping from duty cycle variation to lift coefficient variations had to be approximately inverted, using harmonic balancing. The actuation command used to achieve near sinusoidal lift output was: $DTC(t) = 2.92A\sin(\omega t) + 7.7A^2\sin^2(\omega t)$, where the parameter **A** defines the desired amplitude in the

resultant C_L oscillations. Eq. 5 and figure 6, respectively, show the variant of Eq. 3 with U'=0, and the comparison between the model and experimental measurement.

$$L(t) = \frac{\rho S}{2}\left[C_{Lo}U_o^2 + \underline{C'_L U_o^2}\right] \tag{5}$$

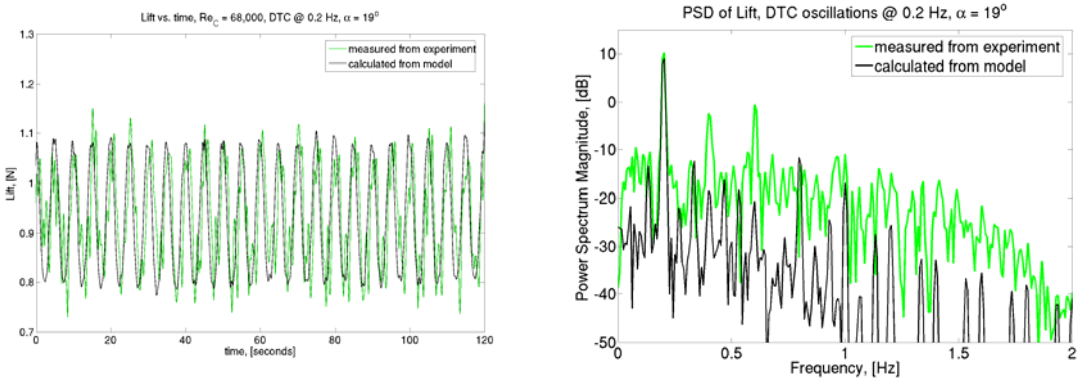

Figure 6. Time series (a) with spectra (b) of lift from experiment and Eq. 5 output for actuation oscillation in a steady freestream.

Again, model output predictions of frequency, amplitude and phase are well matched by experimental measurements. The noticeable peaks beyond the fundamental frequency in Figure 6b are suspected to be due to noise insertion related to the actuation period. The next experiments were conducted using AFC in an attempt to damp freestream induced lift oscillations.

V. Proof of Concept - Feed Forward Control

Using the decompositions of Eq. 2, the purpose of the outer-loop control is both to maintain the desired level of the mean lift L_o and to attenuate, or ideally cancel the fluctuations L'. This translates to using the inner-loop controlled variations of C'_L that cancel the contribution of U' to L' in Eq. 3b. As a proof of concept we check the ability to achieve this goal for a sinusoidal fluctuation in the incoming flow.

After making the substitution of Eq. 2 into Eq. 4, two equations are formed by collecting all mean components into one non-time dependent equation, and all components with at least one "prime" term present into another time dependent equation, Eq. 7.

$$\frac{2}{\rho S}L' = C'_L\left(U_o^2 + 2U_oU' + U'^2\right) + C_{Lo}\left(2U_oU' + U'^2\right) \tag{7}$$

With L' set to zero, Eq. 7 is solved for C'_L, which gives the algorithm for how to operate the valves in response to U'. Depending on which terms are kept, the feed-forward control may attenuate only the fundamental, or the fundamental and its harmonics. In the first cut development of the feed-forward control, all harmonic frequency terms were set to zero, leaving the resulting feed-forward control law to only account for the suppression of the fundamental frequency. Later, the feed-forward control was derived again, leaving the harmonic terms. With these present, the new feed-forward controller actually shows the ability to suppress the higher order frequencies that appear in the power spectrum of the lift. The baseline (no control case) and two controlled cases are shown in figure 7.

It is important to test the inner-loop controller's ability to suppress only the single fundamental frequency, because the fluid dynamics of the flow control process contain many nonlinear effects. It is conceivable that suppression of the fundamental could result in attenuation or enhancement of the first harmonic. Suppressing only a

the fundamental requires that $C_L^{'} = \frac{-2C_{L0}}{U_0}U'$. The results in figure 7 show that suppression of the fundamental at 0.2 Hz also introduces energy to the first harmonic at 0.4 Hz. This effect is predicted by the quasi-static model equation, i.e., the harmonic will increase in energy by $3C_{L0}A^2$. The magenta line in figure 7 shows approximately 10dB increase in energy at the harmonic.

When the control algorithm is modified to suppress both fundamental and harmonic, then required lift coefficient control becomes $C_L' = \frac{-2C_{L0}U'}{U_0 + 2U'}$. The resulting controlled lift spectrum is shown by the solid blue line in figure 7. The attenuation at the fundamental frequency is the same as the previous case, but with this controller energy is not added to the first or second harmonics at 0.4Hz and 0.6Hz. Extraneous peaks appear in the spectra at 0.5Hz, 0.7Hz, and 0.9Hz, which we believe are related to the step-like behavior of the variable duty cycle actuation.

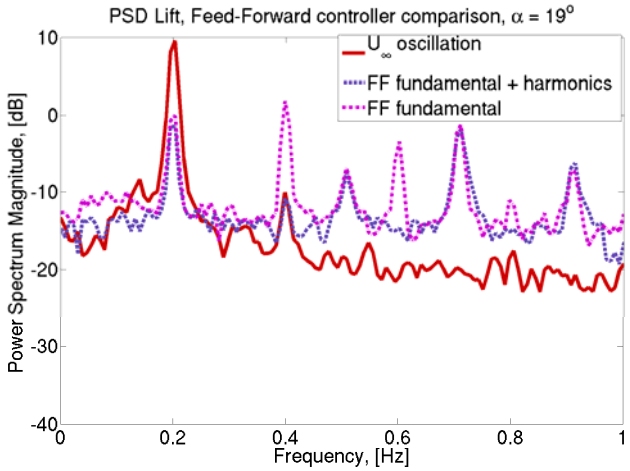

Figure 7. Feed-Forward control with and without higher order frequency suppression capabilities.

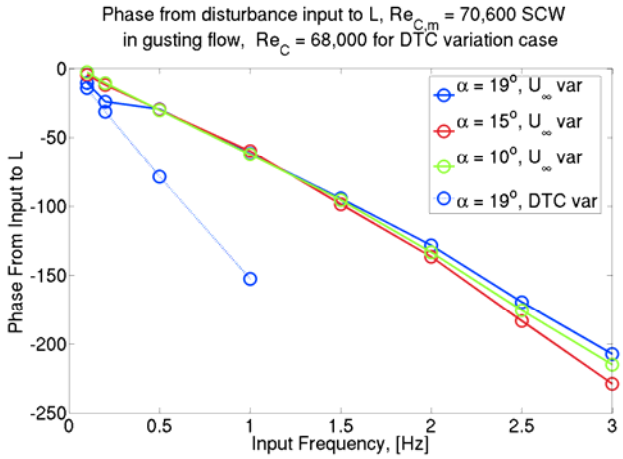

Figure 8. Input–output phase shift dependence on input frequency for the semi-circular wing lift generation.

V.A Time Delays

To better assess the validity of the quasi-steady assumption, measurements of the phase shift between oscillating inputs to the wing (U_∞ and C_L) and the lift output at the fundamental frequency were obtained. In each case, only one quantity was allowed to oscillate, and the phase difference between the lift and the input were assessed. $U_\infty(t)$ measurements were provided by hotwire anemometer. The analog signal driving the pulsed-blowing jet provided the reference signal for the C_L fluctuations. The phase angle between input signals and the lift force were measured at frequencies ranging from 0.1Hz to 3.0Hz. Figure 8 shows the results for the freestream and actuation oscillation cases.

If the quasi-steady approximation was strictly valid, then there would not be a phase variation with frequency. However, we see that already at 0.2 Hz oscillation the lift lags the freestream oscillation by approximately 10°, and the lift lags the actuator input signal by approximately 40°. The difference in the phase lags is not accounted for by the quasi-steady model, which reduces the ability of the control to suppress the lift oscillations.

The slope of the phase to the frequency line gives the time delay. For the lift dependence on freestream speed, the time delay is τ_u = 0.18 seconds for all three angles of attack investigated. When normalized by the freestream speed and the chord τ_u^+=4.8.

It was originally suspected that the presence of a separated flow region on the wing was responsible for the large phase lags in the freestream oscillation case. For this reason, this experiment was operated at a few different angles of attack corresponding from fully attached (α=10°) to

partially stalled conditions (α=15^o and 19^o). Figure 8 shows that the separation region is not responsible for the long delays, because negligible differences are seen when the wing is at 10^o angle of attack.
The duty cycle variation experiments can be operated at frequencies up to 1 Hz, which is shown by the lower line with the steeper slope. In this case the data indicates a significantly increased time constant τ_a=0.43 seconds for the lift response to the actuator input. When normalized by the freestream speed and the chord, τ_a^+ = 11.3.

VI. Conclusion

The eventual goal of this work is to demonstrate enhanced maneuverability of a wing using inner-loop active flow control combined with outer-loop flight control. In this demonstration experiment, an oscillating freestream flow produces an oscillating lift on a fixed wing in a wind tunnel. The ability to attenuate lift oscillations with a feed-forward controller was demonstrated using two control algorithms based on a quasi-steady lift model. The first controller was designed to suppress only the fundamental frequency of oscillation. However, the control algorithm introduced energy into the first and second harmonics. A second controller, also based on the quasi-steady lift model, was used to suppress the fundamental and its harmonics. Approximately 10dB of suppression of the fluctuating lift was achieved at the fundamental frequency with both controllers, but the second controller did not increase the energy of the harmonics. Measurements of the time lags between the lift force and the freestream oscillation, and the lift force and the actuator signal showed significant differences with increasing freestream oscillation frequency. Even at the low oscillation frequency of 0.2 Hz the time delays are important, and if correctly modeled, then more effective control should be achieveable.

Acknowledgments

The support for this work by the U.S. Air Force Office of Scientific Research MURI (FA9550-05-0369) with program manager Dr. Fariba Fahroo is gratefully appreciated. We also acknowledge the support from the Illinois NASA Space Grant Consortium for partial support of Jesse Collins.

References

[1] Colonius, T., Rowley, C.W., Tadmor, G., Williams, D.R., Taira, K., "Closed-loop Control of Leading-edge and Tip Vortices for Small UAV," 1st Donf. On Active Flow Control, Berlin Germany, Sept. 27-29, 2006.

[2]Williams, D., and Collins, J., "Active Concentration of Vorticity Along the Leading Edge of a Semi-Circular Wing," American Physical Society-Div. Fluid Dynamics Abstract, Salt Lake City, Nov. Aug 2007.

[3]Hoblit, F.M., *Gust Loads on Aircraft: Concepts and Applications*, AIAA Education Series, Washington D.C., 1988.

[4]Williams, D.R., Doshi,S., Collins, J., Colonius, T., "Control of the Spanwise Distribution of Circulation on NACA 0012 and Flat Plate Wings," AIAA Paper 2007-1121.